

TABLE II
FOURIER DESCRIPTORS ARE USED; $NF = 4$

$\psi/(\pi/4)$	0.0	0.25	0.5	0.75	1.0	2.0	3.0	7.0
\bar{n}_8	$(\hat{x}_0, \hat{y}_0, \hat{x}_0, \hat{y}_0)$	(5,5,0,6)	2,7,8,12	2,7,12,3	2,7,8,11	(5,5,0,5)	(5,5,0,5)	(5,5,0,5)
	$\hat{\psi}/(\pi/4)$	0.0299	4.6343	4.9979	5.1640	1.0431	2.0431	3.0431
	ρ_{\max}	0.99948	0.99925	0.99823	0.99974	0.99951	0.99951	0.99951
\bar{n}_{16}	$(\hat{x}_0, \hat{y}_0, \hat{x}_0, \hat{y}_0)$	(5,5,0,6)	(5,5,0,7)	(5,5,0,6)	(5,5,0,7)	(5,5,0,6)	(5,5,0,6)	(5,5,0,6)
	$\hat{\psi}/(\pi/4)$	0.0186	0.2791	0.5431	0.7792	1.0431	2.0431	3.0431
	ρ_{\max}	0.99951	0.99926	0.99950	0.99926	0.99950	0.99950	0.99950

TABLE III
FOURIER DESCRIPTORS ARE USED; $\psi = 1.0*(\pi/4)$; $NF = 4$

$R(e, \sigma)$	(0,0.5)	(0,1.0)	(0,2.0)	(0,4.0)	(2.0,3.0)
\bar{n}_8	$(\hat{x}_0, \hat{y}_0, \hat{x}_0, \hat{y}_0)$	(5,5,0,6)	(5,5,0,3)	(5,5,0,3)	(5,5,0,3)
	$\hat{\psi}/(\pi/4)$	1.03565	1.0718	1.08953	1.11666
	ρ_{\max}	0.99947	0.99924	0.99924	0.99876
\bar{n}_{16}	$(\hat{x}_0, \hat{y}_0, \hat{x}_0, \hat{y}_0)$	(5,5,0,4)	(5,5,0,6)	(5,5,0,6)	(2,8,5,5)
	$\hat{\psi}/(\pi/4)$	1.0346	1.02715	1.0171	5.4827
	ρ_{\max}	0.99949	0.99929	0.99876	0.99832

VI. CONCLUSIONS

With the use of Fourier descriptors and the phase correlation function, a previously developed two-level classifier based on multidirectional gradient codes has been extended to deal with the case of unknown angular misalignment. By increasing the number of directional axes, significant reduction in the sensitivity of the estimated position to angular misalignment has been observed. Further Monte Carlo simulation will be required to obtain more explicit results. Various constants, such as H_0 , w_0 , NF , ρ_0 etc., are presently chosen by intuition and are used as "tuning" parameters of our algorithm. However, it should be possible to obtain a set of reasonable estimates using training samples or derived statistics of the $P1$ and $P2$ contour maps. For more accurate angular misalignment determination, the use of prefiltering based on mean-square coherence (MSC) [19] seems to deserve further study.

Although computationally expensive, the present method is useful in two aspects: 1) If a direction indicator is available for proper alignment, a list of points with similar gradient codes but different orientation can be obtained; and 2) if no direction indicator is available, the algorithm is required for both direction finding and position estimation.

REFERENCES

- [1] E. L. Hall, *Computer Image Processing and Recognition*. New York: Academic, 1979, ch. 8.
- [2] D. I. Barnea and H. F. Silverman, "A class of algorithms for fast image registration," *IEEE Trans. Comput.*, vol. C-21, pp. 172-186, 1972.
- [3] J. P. Golden, "Terrain contour matching (TERCOM): A cruise missile guidance aid," in *Proc. SPIE Image Processing Missile Guidance*, vol. 238, pp. 10-18, 1980.
- [4] R. D. Andreas, L. D. Hostetler, and R. C. Beckmann, "Continuous Kalman updating of an inertial navigation system using terrain measurements," in *Proc. IEEE NAECON*, 1978, pp. 1263-1270.
- [5] A. M. Savol, A. J. Witsmeier, E. Noges, and J. Geros, "Development of an onboard navigational update system utilizing pattern recognition," in *IEEE Conf. Pattern Recognition Image Processing*, 1978, pp. 91-95.
- [6] K. P. Lam, "Position determination using generalized multidirectional gradient codes," *Comput. Vision, Graphics, Image Processing*, vol. 28, pp. 228-239, 1984.
- [7] S. P. Morse, "Computer storage of contour-map data," in *Proc. 23rd Ass. Comput. Mach. Nat. Conf.*, 1968, pp. 45-51.
- [8] H. Freeman and S. P. Morse, "On searching a contour map for a given terrain elevation profile," *J. Franklin Inst.*, vol. 248, pp. 1-25, 1967.
- [9] R. D. Merrill, "Representation of contours and regions for efficient computer search," *Comm. Ass. Comput. Mach.*, vol. 16, pp. 69-82, 1973.
- [10] H. T. Tsui and K. P. Lam, "On the problem of classification of weather contour maps," in *Proc. 4th Int. Conf. Pattern Recognition*, 1978, pp. 635-637.
- [11] K. P. Lam, "A syntactic method of weather pattern recognition," M.Phil. thesis, Chinese Univ., Hong Kong, 1977.
- [12] D. Y. Montuno, Y. Yoshida, and T. Fukumura, "Structural description of contour maps and its application to weather maps," *Trans. IECE Japan*, vol. E63, pp. 421-428, 1980.
- [13] R. Tamiguchi, M. Yokota, E. Kawaguchi, and T. Tamati, "Picture understanding and retrieving system of weather chart," in *Proc. 6th Int. Conf. Pattern Recognition*, 1982, pp. 802-805.
- [14] H. Freeman and J. A. Saghi, "Comparative analysis of line-drawing modeling schemes," *Comput. Graphics Image Processing*, vol. 12, pp. 203-223, 1980.
- [15] E. Persoon and K. S. Fu, "Shape discrimination using Fourier descriptors," *IEEE Trans. Syst., Man, Cybern.*, vol. SMC-7, pp. 170-179, 1977.
- [16] J. S. Bendat and A. G. Piersol, *Random Data: Analysis and Measurement Procedures*. New York: Wiley-Interscience, 1971, ch. 1.
- [17] C. D. Kuglin, A. F. Blumenthal, and J. J. Pearson, "Map-matching techniques for terminal guidance using Fourier phase information," in *Proc. SPIE Digital Processing Aerial Images*, vol. 186, 1979, pp. 21-29.
- [18] R. C. Gonzalez and P. Wintz, *Digital Image Processing*. Reading, MA: Addison-Wesley, 1977, ch. 3.
- [19] G. C. Carter, Ed., Special Issue on Time Delay Estimation, *IEEE Trans. Acoust., Speech, Signal Processing*, vol. ASSP-29, pp. 461-621, 1981.

Template Matching in Rotated Images

ARDESHIR GOSHTASBY

Abstract—A rotationally invariant template matching using normalized invariant moments is described. It is shown that if normalized invariant moments in circular windows are used, then template matching in ro-

Manuscript received November 28, 1983; revised December 17, 1984. Recommended for acceptance by S. L. Tanimoto.

The author is with the Department of Computer Science, University of Kentucky, Lexington, KY 40506.

tated images becomes similar to template matching in translated images. A speedup technique based on the idea of two-stage template matching is also described. In this technique, the zeroth-order moment is used in the first stage to determine the likely match positions, and the second- and third-order moments are used in the second stage to determine the best match position among the likely ones.

Index Terms—Image registration, invariant moments, Mann-Whitney test, satellite imagery, two-stage template matching.

I. INTRODUCTION

Template matching is the process of determining the position of a template inside an image. This process is used as the basic step in many image registration techniques. One way to register two images is to select a set of windows (templates) from one image and try to locate the windows in the other image. Then, using the coordinates of the centers of corresponding windows in the two images, the registration parameters are determined [1], [2].

Major similarity measures that are used in template matching are the sum of absolute differences and the cross-correlation coefficient. The sum of absolute differences is computationally fast [2], but the correlation coefficient measure is more accurate [3]. Other similarity measures have also been used in the window search process such as Haar transform coefficients [4], Walsh-Hadamard transform coefficients [5], and invariant moments [6].

If the images are rotated with respect to each other, none of the above similarity measures can be used. This is because, even though the centers of two windows correspond to each other, other points in the windows do not correspond to each other, and a low similarity measure might be obtained. As a matter of fact, similarity measure is not the only problem. When two images are rotated with respect to each other, it is impossible for two rectangular windows to contain the same parts of the scene (except when the two windows are rotated by a multiple of 90° with respect to each other). To overcome this problem, we should take circular windows. Then, when the centers of two windows correspond to each other, they will cover the same areas of the scene no matter what the rotational difference between them.

In Section II, template matching in rotated images using normalized invariant moments and circular windows is discussed. Normalized invariant moments are used to compute the similarity between circular windows. Since computation of invariant moments is very time consuming, in Section III a two-stage search process which uses the zeroth-order moment in the first stage to determine the likely positions for a match, and uses the second- and third-order moments in the second stage to determine the best match position among the likely ones, is described. Finally, in Section IV, the results of the proposed technique on real and generated images are given. In the following sections, moments, central moments, invariant moments, normalized moments, normalized central moments, and normalized invariant moments are denoted by m , u , a , M , U , and A , respectively.

II. INVARIANT MOMENTS

The two-dimensional $(p+q)$ th order moment of a digital image f is defined by

$$m_{pq} = \sum_x \sum_y x^p y^q f(x, y). \quad (1)$$

where $f(x, y)$ is the pixel value of image f at location (x, y) [7].

Measure m_{pq} changes if f is translated. To make m_{pq} invari-

ant with respect to translation of f , (1) is modified as below,

$$u_{pq} = \sum_x \sum_y (x - \bar{x})^p (y - \bar{y})^q f(x, y) \quad (2)$$

where

$$\bar{x} = \sum_x \sum_y x f(x, y) / \sum_x \sum_y f(x, y) = m_{10} / m_{00}$$

$$\bar{y} = \sum_x \sum_y y f(x, y) / \sum_x \sum_y f(x, y) = m_{01} / m_{00}$$

u_{pq} is called the $(p+q)$ th order central moment of image f and is invariant with respect to the translation of image f [7].

We still cannot apply u_{pq} in the template matching process because u_{pq} varies with respect to the rotation of image f . Hu has been able to derive moments that are invariant with respect to rotation of an image [7]. The second-order and third-order moments which are invariant with respect to the rotation and translation of image f are [7]

$$a_1 = u_{20} + u_{02} \quad (3)$$

$$a_2 = (u_{20} - u_{02})^2 + 4u_{11}^2 \quad (4)$$

$$a_3 = (u_{30} - 3u_{12})^2 + (3u_{21} - u_{03})^2 \quad (5)$$

$$a_4 = (u_{30} + u_{12})^2 + (u_{21} + u_{03})^2 \quad (6)$$

$$a_5 = (u_{30} - 3u_{12})(u_{30} + u_{12})[(u_{30} + u_{12})^2 - 3(u_{21} + u_{03})^2] + (3u_{21} - u_{03})(u_{21} + u_{03})[3(u_{30} + u_{12})^2 - (u_{21} + u_{03})^2] \quad (7)$$

$$a_6 = (u_{20} - u_{02})[(u_{30} + u_{12})^2 - (u_{21} + u_{03})^2] + 4u_{11}(u_{30} + u_{12})(u_{21} + u_{03}) \quad (8)$$

$$a_7 = (3u_{21} - u_{03})(u_{30} + u_{12})[(u_{30} + u_{12})^2 - 3(u_{21} + u_{03})^2] - (u_{30} - 3u_{12})(u_{21} + u_{03})[3(u_{30} + u_{12})^2 - (u_{21} + u_{03})^2]. \quad (9)$$

Usually more than one moment is used in decision making. One way to measure similarity between two windows is to compute the distance between two vectors of moments from the windows. The smaller the distance, the more similar the two windows [8]. This method, however, requires that the feature elements in the vectors be of the same scale. Moments of different orders do not have the same scale. The correlation of the logarithm of moments has been used to measure the similarity between two windows [6]. Again, the moments of different orders have different scales and using the logarithm of the moments would not solve the problem. The correlation between two sets of features is defined when the feature values in each set are of the same scale. When features of different scales are used in the computation of correlation, the feature with the largest scale will dominate the correlation value.

Garrett has proposed the concept of pairing functions where the similarity between two sets of features is determined by quantizing the features and counting the number of quantized features that are equal [9]. In this technique, since the features in a set are quantized into the same number of levels, it is as if the features are measured with the same scale. This alleviates the problem of scale differences but causes loss of some information in the quantization process. When the feature values are quantized, critical information needed in the measurement of similarity may disappear.

To overcome this problem, in the following, the moments of all orders are normalized so that they have the same scale.

TABLE I
ORIGINAL MOMENTS AND NORMALIZED MOMENTS OF WINDOW OF FIG. 1

MOMENTS	ORIGINAL	NORMALIZED
M(0,0)=	0.1241500E+05	0.1241500E+05
M(0,1)=	0.1071010E+06	0.1127379E+05
M(1,0)=	0.9822100E+05	0.1033906E+05
M(0,2)=	0.1208743E+07	0.1339328E+05
M(1,1)=	0.8615781E+06	0.9546570E+04
M(2,0)=	0.1046483E+07	0.1159538E+05
M(0,3)=	0.1527869E+08	0.1782032E+05
M(1,2)=	0.9858765E+07	0.1149878E+05
M(2,1)=	0.9134983E+07	0.1065460E+05
M(3,0)=	0.1274178E+08	0.1486139E+05
M(0,4)=	0.2049458E+09	0.2516197E+05
M(1,3)=	0.1259041E+09	0.1545771E+05
M(2,2)=	0.1043736E+09	0.1281434E+05
M(3,1)=	0.1097818E+09	0.1347832E+05
M(4,0)=	0.1667723E+09	0.2047527E+05
M(0,5)=	0.2851797E+10	0.3685538E+05
M(1,4)=	0.1701998E+10	0.2199588E+05
M(2,3)=	0.1333064E+10	0.1722793E+05
M(3,2)=	0.1245624E+10	0.1609789E+05
M(4,1)=	0.1416772E+10	0.1830973E+05
M(5,0)=	0.2283082E+10	0.2950553E+05

The normalized moment of order $(p+q)$ for image f with dimensions $N \times N$ is defined by

$$M_{pq} = \sum_x \sum_y (x/x')^p (y/y')^q f(x, y)$$

where

$$x' = (1/N) \sum_{x=1}^N x = N(N+1)/2N = (N+1)/2$$

$$y' = (1/N) \sum_{y=1}^N y = (N+1)/2.$$

So, actually

$$\begin{aligned} M_{pq} &= \sum_{x=1}^N \sum_{y=1}^N \{x/[(N+1)/2]\}^p \{y/[(N+1)/2]\}^q f(x, y) \\ &= [2/(N+1)]^{p+q} \sum_x \sum_y x^p y^q f(x, y) \\ &= [2/(N+1)]^{p+q} m_{pq}. \end{aligned}$$

The normalized $(p+q)$ th order moment is equal to the $(p+q)$ th order moment multiplied by the scaling factor $[2/(N+1)]^{p+q}$. Table I shows the normalized moments for the window of Fig. 1.

To determine the normalized central moments, we replace x by $x/[(N+1)/2]$ and y by $y/[(N+1)/2]$ in formula (2). Or,

$$\begin{aligned} U_{pq} &= \sum_x \sum_y \{(x-x)/[(N+1)/2]\}^p \\ &\quad \cdot \{(y-y)/[(N+1)/2]\}^q f(x, y) \\ &= [2/(N+1)]^{p+q} \sum_x \sum_y (x-x)^p (y-y)^q f(x, y) \\ &= [2/(N+1)]^{p+q} u_{pq}. \end{aligned}$$

In the same manner we can determine the normalized invariant moments from formulas (3)-(9) as shown below.

$$A_1 = [2/(N+1)]^2 a_1 \quad (10)$$

$$A_2 = [2/(N+1)]^4 a_2 \quad (11)$$

$$A_3 = [2/(N+1)]^6 a_3 \quad (12)$$

$$A_4 = [2/(N+1)]^8 a_4 \quad (13)$$

	0	1	2	3	4	5	6	7	8	9	10	11	12	13	14	15
0	71	65	68	67	64	65	66	65	65	66	65	68	64	60	59	
1	68	65	67	67	62	62	66	67	67	63	61	60	55	50	44	43
2	68	67	66	62	60	64	66	66	61	51	45	44	41	38	38	38
3	66	66	62	65	67	60	56	51	40	35	33	33	34	36	38	37
4	64	67	65	67	60	46	39	40	35	38	40	42	45	40	43	43
5	64	66	60	49	38	32	33	40	46	53	51	54	56	61	62	65
6	66	60	45	33	30	35	38	45	49	57	59	57	65	73	74	77
7	54	39	34	30	29	34	36	44	52	55	59	68	71	72	75	77
8	42	28	26	28	30	31	35	37	43	49	53	57	64	70	73	74
9	35	31	29	31	30	28	32	34	39	44	49	53	60	65	71	72
10	37	38	33	34	35	29	27	30	33	35	42	50	56	59	63	70
11	42	41	38	37	35	31	30	33	32	35	35	40	48	52	59	67
12	44	42	44	39	36	35	37	38	33	35	34	36	42	47	53	61
13	49	45	48	46	40	38	39	35	36	35	38	35	37	38	45	48
14	52	56	51	47	41	41	40	37	36	37	36	37	35	37	41	46
15	63	56	53	48	46	44	46	44	39	40	39	35	36	39	42	

Fig. 1. A 16×16 window.

$$A_5 = [2/(N+1)]^{12} a_5 \quad (14)$$

$$A_6 = [2/(N+1)]^8 a_6 \quad (15)$$

$$A_7 = [2/(N+1)]^{12} a_7. \quad (16)$$

In the following, the normalized invariant moments from two circular windows will be used as features to determine the similarity between two windows.

III. TWO-STAGE TEMPLATE MATCHING

Template matching is the process of determining the position of a subimage inside a larger image. The subimage is called the template and the larger image is called the search area. The template matching process involves shifting the template over the search area and computing the similarity between the template and the window in the search area over which the template lies. The next step is determining the shift position where the largest similarity measure is obtainable. This is the position in the search area where the template is most likely to be located.

To determine the similarity between two windows, eight normalized invariant moments from the two windows are used. These are: one zeroth-order, three second-order, and four third-order normalized invariant moments. The zeroth-order normalized invariant moment is equal to the sum of the intensity values in a window,

$$A_0 = \sum_x \sum_y f(x, y) \quad (17)$$

where $f(x, y)$ is the intensity value at position (x, y) in the window. The second and third-order normalized invariant moments are (A_1, A_2, A_3) and (A_4, A_5, A_6, A_7) , respectively [see (10)-(16)]. Assuming A_0, A_1, \dots, A_7 and B_0, B_1, \dots, B_7 are two sets of normalized invariant moments from two different windows, adjusted such that each set has a mean of zero, then the similarity between the windows can be determined by the cross-correlation of the moments.

$$r = \frac{\sum_{i=0}^7 A_i B_i}{\left[\sum_{i=0}^7 A_i^2 \sum_{i=0}^7 B_i^2 \right]^{1/2}} \quad (18)$$

r changes between -1 and $+1$, and the closer r is to $+1$, the more similar the two windows will be. r should be computed for every shift position and this involves computation of the eight normalized invariant moments for every position which is a very time consuming process.

To speed up this process, a two-stage technique has been developed. Two-stage template matching has previously been used on translated images [10]-[12]. The main idea in two-stage template matching has been to use a subtemplate in the first stage to determine the likely positions in the search area where the template might exist, and use the whole template

in the second stage to determine the best match among the likely ones.

Based on the same idea, a two-stage template matching technique is developed such that it could be applied to translated and rotated images. In this approach, first a fast similarity measure (the zeroth-order moment) is used to determine the likely positions for a match. Then, an accurate but slower similarity measure (using the second- and third-order moments) is used to determine the best match among the likely ones. The important problem in two-stage template matching is the determination of the threshold value which decides the likely matches. In the following, given a false dismissal probability, the threshold value of the first stage is determined.

A. Threshold Estimation

It is assumed that the template and the best match window have about the same mean. If the template and the search area are obtained under different lighting conditions or with different sensors, an image intensity transformation is required to transform the intensity of one image to the intensity of another image [13].

Now, if a template truly matches with a window in the search area, then the window and the template will have approximately the same mean. Conversely, if the mean of the template and a window are considerably different, then it is unlikely that they will match. This will be the selection criterion for the first stage. If the difference between the mean of the template and a given window is greater than a threshold value, we decide that the template is unlikely to match with the given window with a false dismissal probability. However, if the means of the template and a window are approximately the same, it does not necessarily imply that the template and the window match. Among the likely matches, higher order moments will be used to select the best match. Rather than using the zeroth-order moment for a window, we use its mean. The mean of a window is obtained by dividing the zeroth-order moment by the number of pixels in the window.

Since the underlying distributions of the template and windows in the search area are usually not known, the Mann-Whitney test will be used to determine whether the underlying distributions for a given template and a given window have the same mean [14]. The Mann-Whitney test is applied to two randomly selected samples that are mutually independent and independency within each sample also holds. Using the template and a window from the search area as two samples, the condition of independency between samples holds but the condition of independency within samples may not hold. This is because the intensities in an image usually change gradually rather than randomly. To be able to approximate independency within samples, we select templates from nonhomogeneous areas, and rather than taking the whole template as a sample, a randomly selected sample is used.

If the sample is too large, the condition of independency within samples may not hold. If the sample is too small, it may not represent the window or the template well. Assuming N is the number of pixels in the window or the template, it has been found experimentally that the number of points in a sample equal to $N/16-N/4$ is appropriate.

The test statistics for the Mann-Whitney test is the sum of the ranks assigned to the sample from the template

$$T = \sum_{i=1}^n R(X_i) \quad (19)$$

where n is the number of sample points in the template and $R(X_i)$ is the rank of sample point X_i when both samples are used in ranking [14]. If more than one sample point has the same value (ties), we should assign to each the average of the ranks that would have been assigned to them had there been

TABLE II
JOINT RANK ORDER FOR TWO SAMPLES X AND Y

X	42	56	63	73		90	106	125	129	148	161									
Y	24		62	64	76	79	99	106	127	142		169								
R	1	2	3	4	5	6	7	8	9	10	11	12.5	12.5	14	15	16	17	18	19	20

no ties [14]. Formula (19) is for the case where there are no, or just a few, ties in the sample. If there are many ties, T should be normalized [14, p. 216].

The decision rule is to reject the null hypothesis (the hypothesis that the two samples belong to two distributions with the same mean) at the level of significance α if

$$T < w_{\alpha/2} \quad \text{or} \quad T > w_{1-\alpha/2}$$

and accept the null hypothesis if

$$w_{\alpha/2} \leq T \leq w_{1-\alpha/2}$$

where $w_{\alpha/2}$ and $w_{1-\alpha/2}$ are the $\alpha/2$ and $(1-\alpha/2)$ quantiles, respectively, and are tabulated for different values of α and n .

An Example: Let two random samples of size 10 from the template and the window be as follows.

Sample from the template

X : 148, 73, 56, 63, 90, 42, 106, 125, 129, 161.

Sample from the window

Y : 127, 169, 76, 24, 62, 99, 142, 79, 106, 64.

The ranking is shown in Table II, and

$$T = \sum_{i=1}^{10} R(X_i)$$

$$= 2 + 3 + 5 + 7 + 10 + 12.5 + 14 + 16 + 18 + 19 = 106.5.$$

For $n = 10$ and assuming $\alpha = 0.01$, we find $w_{\alpha/2} = 72$ and $w_{1-\alpha/2} = 138$. Since $72 < T < 123$, we cannot reject the null hypothesis and, therefore, the two underlying distributions from which the samples were taken have the same mean with minimum guaranteed probability 0.99.

To summarize, we determine the windows that are likely to match with the template as follows. For each window and the template, 1) take a random sample of size n from each of the template and the window. 2) Rank order the two samples jointly. 3) Compute the test statistics T by adding the ranks of sample points in the template. 4) If $T < w_{\alpha/2}$ or $T > w_{1-\alpha/2}$ then it is unlikely that the template and the window match with false dismissal probability α . Otherwise, (when $w_{\alpha/2} \leq T \leq w_{1-\alpha/2}$) the window and the template are likely to match.

This procedure will select the windows that are likely to match with the template. These windows will be used in the second stage to determine the best match.

IV. RESULTS

To verify the validity of the proposed two-stage template matching process, two experiments were carried out. In the first experiment, a search area of radius 16 was generated (see Fig. 2). A window of radius 8, as shown in Fig. 2, was taken from the search area, rotated by 45° and random noise was generated from a uniform distribution over $(-\sigma, \sigma)$ and added to it, where σ is the standard deviation of the window (see Fig. 3). This is assumed to be the template.

The template is shifted over the search area and, using the procedure of Section III-A, the likely positions for a match are determined, as shown in Fig. 4. The O's show the shift positions where the Mann-Whitney test rejects the null hypothesis and, therefore, are unlikely to be the match positions

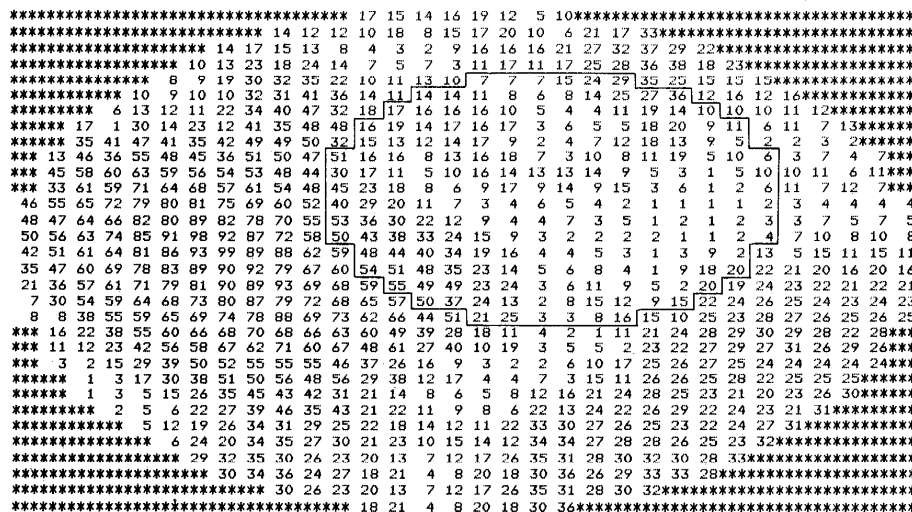


Fig. 2. A search area of radius 16.

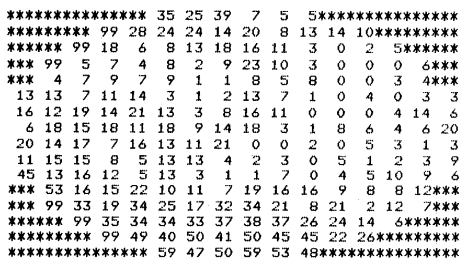


Fig. 3. A template of radius 8.

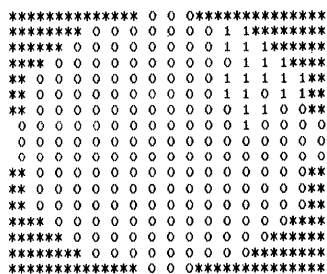


Fig. 4. The result of the first stage. Only those cases shown by the 1's should be tested in the second stage.

with $\alpha = 0.01$. The positions shown by 1's are the only ones remaining and should be tested in the second stage to determine the best match position.

The experiment was carried out 100 times, each time with a different initial value for the noise generator. In all cases, the best match position remained among the likely match positions in the first stage. On the average, 22.0 windows were found to be good candidates for a match, and therefore needed to be tested in the second stage.

In the second experiment, amplitude of noise was increased by a factor of 2 [noise was generated over $(-2\sigma, 2\sigma)$], and the same procedure was repeated. Again, the best match position was not missed in the first stage. The average number of posi-

TABLE III
RESULTS OF THE FIRST STAGE IN THE TWO-STAGE TEMPLATE MATCHING PROCESS FOR 100 TRIALS, $\alpha = 0.01$

	Amount of noise	# of times the best-match was missed.	Average # windows likely to be the best-match, X .
Experiment 1	$(-\sigma, \sigma)$	0	22.0
Experiment 2	$(-2\sigma, 2\sigma)$	0	25.2

tions needed to be tested in the second stage was determined to be 25.2. The results of the two experiments are summarized in Table III.

Assuming the template is $N \times N$ and the search area is $M \times M$, then the number of windows in the search area that should be matched with the template is $(M - N + 1)^2$. Assuming computation of the Mann-Whitney test for each shift position takes R seconds, and computation of the eight invariant moments and measurement of similarity using these moments for every shift position takes S seconds, and assuming in the first stage X windows are found to be likely to match with the template, the overall computation time when the one-stage process is used is

$$T1 = (M - N + 1)^2 S$$

while when the two-stage process is used, it is

$$T2 = (M - N + 1)^2 R + XS.$$

Since computation of the first stage is negligible with respect to the computation of the second stage, we can write

$$T2 \approx XS$$

and therefore the speedup factor of the two-stage process compared to the one-stage process is

$$T1/T2 \approx (M - N + 1)^2/X.$$

Using the values of X from Table III, and using $M = 32$ and $N = 16$, we obtain

$$\begin{aligned} \text{speedup factor for Experiment 1} \\ = (32 - 16 + 1)^2/22.0 = 13.1, \end{aligned}$$



Fig. 5. GOES thermal-IR image of Michigan acquired on June 24, 1979. Arrows show the centers of circular templates of radius 8 selected for matching.

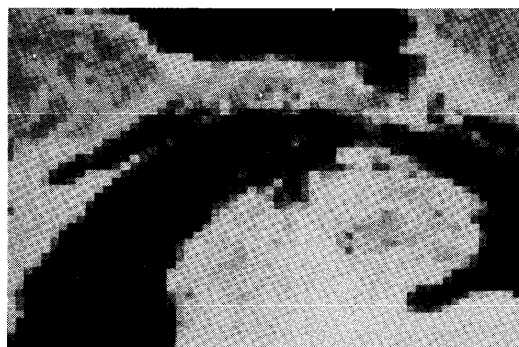


Fig. 6. HCMM day-visible image of Michigan acquired on September 26, 1979.

and

$$\text{speedup factor for Experiment 2} \\ = (32 - 16 + 1)^2 / 25.2 = 11.5.$$

To test the above two-stage template matching process on real data, the following experiment was carried out. Two images from two different satellites were used. Fig. 5 shows a thermal-infrared image of Michigan obtained by the Geostationary Operational Environment Satellite (GOES) on June 24, 1979 at 3:00 P.M. Fig. 6 is a day-visible image of approximately the same area obtained by the Heat Capacity Mapping Mission (HCMM) satellite on September 26, 1979. Both images were already geometrically corrected. The original HCMM image had a 500×500 m resolution. Since the GOES image had a 8×11 km resolution, the HCMM image was smoothed in 16×22 neighborhoods and was resampled at the same resolution as the GOES image. The two images now have the same scale but have translational and rotational differences. Since the two images have been obtained by different sensors, procedure of [13] was used to transform intensities of the GOES image to those of the HCMM image.

Six points located at high variance areas of the GOES image with coordinates (12, 21), (23, 25), (33, 13), (35, 30), (47, 20), and (46, 35) were selected, (see Fig. 5). Circular templates with



Fig. 7. GOES image resampled to overlay with the HCMM image.

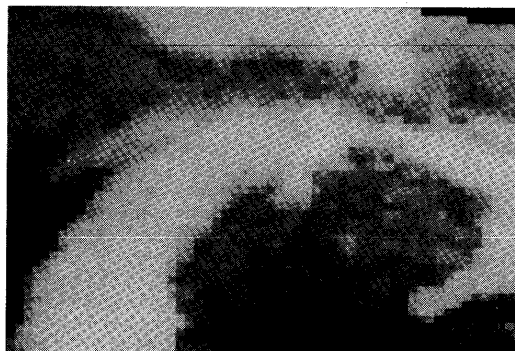


Fig. 8. GOES and HCMM images registered.

an 8-pixel radius were taken centered at the selected points. The templates were searched in the HCMM image using the proposed two-stage template matching technique. Corresponding windows were determined to be centered at (16, 21), (27, 37), (39, 17), (38, 35), (51, 27), and (47, 42). The centers of corresponding templates and windows were then used in the RANSAC (random sample consensus) procedure to determine the registration parameters [15]. The RANSAC procedure first eliminates the mismatches and then determines the registration parameters using the remaining corresponding points and the least-squares technique.

Using the transformation,

$$x' = x \cos \theta - y \sin \theta + h \\ y' = x \sin \theta + y \cos \theta + k$$

with (x', y') and (x, y) showing the coordinates of corresponding points in the HCMM and GOES images, respectively, the parameters were determined to be: $\theta = 11.5^\circ$, $h = 9.40$ pixels, and $k = -1.38$ pixels.

The GOES image was resampled by the nearest neighbor rule and the transformation

$$x' = 0.98x - 0.20y + 9.40 \\ y' = 0.20x + 0.98y - 1.38.$$

The resampled image is shown in Fig. 7. The resampled GOES image is negated and is overlaid with the HCMM image in Fig. 8 to visualize the registration. The accuracy of the template matching technique in locating corresponding points in the images is summarized in Table IV. Most errors are less than one pixel.

TABLE IV
SQUARE-ROOT ERRORS OF THE SIX CORRESPONDING POINTS FROM THE
GOES AND HCMM IMAGES

No.	Corresponding points in GOES image	HCMM image	Square-root errors
1	(12, 21)	(16, 21)	1.13
2	(23, 25)	(27, 37)	0.06
3	(33, 13)	(39, 17)	0.15
4	(35, 30)	(38, 35)	0.30
5	(47, 20)	(51, 27)	0.77
6	(46, 35)	(47, 42)	0.49

An alternative to the above approach for registration of rotated images is the symbolic approach. In the symbolic approach, the images are segmented and symbolic features such as straight edges [16], connected edges [17], or closed boundary regions [18] are selected from the images. Then by matching these features, image registration is accomplished. The disadvantage of the symbolic approach compared to the template matching approach is that the symbolic approach is scene dependent and in some scenes we may not obtain enough features to match while in others we may obtain too many features that are hard to match. The template matching technique, however, works independent of a scene's content.

V. CONCLUSION

Images that have rotational differences can be registered via a template matching process which uses circular templates and normalized invariant moments. If a small false dismissal probability is allowed, the matching process can be speeded up by dividing the matching process into two stages. In the first stage, the zeroth-order moment is used to determine the likely match positions, and in the second stage the second- and third-order moments are used to select the best match position among the likely ones. The practicality of this process in registration of digital images was demonstrated through registration of two satellite images having known scaling but unknown translational and rotational differences.

ACKNOWLEDGMENT

The author would like to thank the Center for Remote Sensing of Michigan State University, East Lansing, for providing data for this work. The help of Ms. J. Spanyer in preparation of this paper is also appreciated.

REFERENCES

- [1] P. E. Anuta, "Digital image registration of multi-spectral video imagery," *Soc. Photo-Opt. Instrum. Eng. J.*, vol. 7, pp. 168-175, Sept. 1969.
- [2] D. I. Barnea and H. F. Silverman, "A class of algorithms for fast digital image registration," *IEEE Trans. Comput.*, vol. C-21, pp. 179-186, Feb. 1972.
- [3] M. Svedlow, C. D. McGillem, and P. E. Anuta, "Experimental examination of similarity measures and processing methods used for image registration," presented at Symp. Machine Processing Remotely Sensed Data, 1976.
- [4] D. V. S. Chandra, J. S. Boland, W. W. Malcolm, and H. S. Ranganath, "Feature matching multiple image registration using Haar coefficients," in *Proc. SOUTHCON*, Apr. 5-7, 1982, pp. 549-552.
- [5] H. Schutte, S. Frydrychowicz, and J. Schroder, "Scene matching with translation invariant transforms," in *Proc. 5th Int. Joint Conf. Pattern Recognition*, 1980, pp. 195-98.
- [6] R. Y. Wong and E. L. Hall, "Scene matching with invariant moments," *Comput. Graphics Image Processing*, vol. 8, pp. 16-24, 1978.
- [7] M.-K. Hu, "Visual pattern recognition by moment invariants," *Trans. Inform. Theory*, pp. 179-187, 1962.
- [8] V. E. Giuliano, P. E. Jones, G. E. Kimball, R. F. Meyer, and B. Stein, "Automatic pattern recognition by Gestalt method," *Inform. Contr.*, vol. 4, pp. 332-445, 1961.
- [9] G. S. Garret, E. L. Reagh, and E. B. Hibbs, Jr., "Detection threshold estimation for digital area correlation," *IEEE Trans. Syst., Man, Cybern.*, vol. SMC-1, pp. 65-70, 1976.
- [10] G. J. Vanderburg and A. Rosenfeld, "Two-stage template matching," *IEEE Trans. Comput.*, vol. C-26, pp. 384-393, Apr. 1977.
- [11] A. Rosenfeld and G. J. Vanderburg, "Coarse-fine template matching," *IEEE Trans. Syst., Man, Cybern.*, vol. SMC-2, pp. 104-107, Feb. 1977.
- [12] A. Goshtasby, S. H. Gage, and J. F. Bartholic, "A two-stage cross-correlation approach to template matching," *IEEE Trans. Pattern Anal. Machine Intell.*, vol. PAMI-6, pp. 374-378, May 1984.
- [13] R. Y. Wong and E. L. Hall, "Image intensity transformation," in *IEEE Proc. Pattern Recognition Image Processing*, pp. 96-99, 1978.
- [14] W. J. Conover, *Practical Nonparametric Statistics*. New York: Wiley, 1980, pp. 216-223.
- [15] M. A. Fischler and R. C. Bolles, "Random sample consensus: A paradigm for model fitting with application to image analysis and automated cartography," *Comm. ACM*, vol. 24, no. 6, pp. 381-395, 1981.
- [16] G. C. Stockman, S. Kopstein, and S. Bennet, "Matching images to models for registration and object detection via clustering," *IEEE Trans. Pattern Anal. Machine Intell.*, vol. PAMI-4, pp. 229-241, May 1982.
- [17] C. S. Clark, D. K. Conti, W. O. Eckhart, T. A. McCulloh, R. Nevatia, and D. Y. Tseng, "Matching of natural terrain scenes," in *5th Int. Joint Conf. Pattern Recognition*, 1980, pp. 217-222.
- [18] A. Goshtasby, A. K. Jain, and W. R. Enslin, "Automatic digital image registration," in *5th Int. Symp. Mach. Processing Remotely Sensed Data*, 1982, pp. 347-352.

Linear Quadrees from Vector Representations of Polygons

DAVID M. MARK AND DAVID J. ABEL

Abstract—A new algorithm is presented which produces various forms of linear quadrees directly from a vector representation of a polygon. This algorithm takes advantage of specific properties of linear quadrees and associated linear keys to infer the colors of all parts of the region not cut by the polygon boundary. The method is further extended to multicolored (rather than binary) linear quadrees which may be useful in geographic information systems applications.

Index Terms—Geographic information system, quadtree.

I. INTRODUCTION

A *quadtree* represents a digital image of a square region by hierarchically partitioning the region into quadrants and sub-quadrants until all subquadrants are uniform with respect to image value. This approach to image representation was first proposed by Klinger [1], [2]. Conceptually, the hierarchy of quadrants can be considered to be a tree of out-degree four, rooted at a node representing the entire region; such a tree has

Manuscript received February 6, 1984; revised January 10, 1985. Recommended for acceptance by S. L. Tanimoto. This work was supported in part by CSIRO Division of Computing Research.

D. M. Mark was a Visiting Scientist with the CSIRO Division of Computing Research. He is now with the Department of Geography, State University of New York, Buffalo, NY 14260.

D. J. Abel is with the CSIRO Division of Computing Research, Davies Laboratory, Queensland 4814, Australia.